Research Reports: Biological

Osteochondral Interface Stiffening in Mandibular Condylar Osteoarthritis

J. Zhang[1]*, L. Liao[1,2]*, J. Zhu[3]*, X. Wan[1]*, M. Xie[1], H. Zhang[1], M. Zhang[1], L. Lu[1], H. Yang[1], D. Jing[4], X. Liu[1], S. Yu[1], X.L. Lu[5], C. Chen[6], Z. Shan[3], and M. Wang[1] (iD)

Abstract

Osteoarthritis (OA) of the temporomandibular joint (TMJ) is associated with dental biomechanics. A major change during OA progression is the ossification of the osteochondral interface. This study investigated the formation, radiological detectability, and mechanical property of the osteochondral interface at an early stage, the pathogenesis significance of which in OA progression is of clinical interest and remains elusive for the TMJ. Unilateral anterior crossbite (UAC) was performed on 6-wk-old rats as we previously reported. TMJs were harvested at 4, 12, and 20 wk. The progression of TMJ OA was evaluated using a modified Osteoarthritis Research Society International (OARSI) score system. Osteochondral interface was investigated by quantifying the thickness via von Kossa staining of histological slices and in vivo calcium deposition by calcein injection. Tissue ossification was imaged by micro–computed tomography (CT). Mechanical properties were measured at nanoscale using dynamic indentation. Time-dependent TMJ cartilage lesions were elicited by UAC treatment. Geometric change of the condyle head and increased value of the OARSI score were evident in UAC TMJs. At the osteochondral interface, there was not only enhanced deep-zone cartilage calcification but also calcium deposition at the osseous boundary. The thickness, density, and stiffness of the osteochondral interface were all significantly increased. The enhanced ossification of the osteochondral interface is a joint outcome of the aberrant deeper cartilage calcification at the superior region and promoted formation of subchondral cortical bone at the inferior region. The micro-CT detectable ossification from an early stage thus is of diagnostic significance. Although the environment of the cartilage and subchondral bone could be changed due to the stiffness of the interface, whether or not the stiffened interface would accelerate OA progress remains to be confirmed. With that evidence, the osteochondral interface could be a new diagnostic and therapeutic target of the mechanically initiated OA in the TMJ.

Keywords: temporomandibular joint, experimental animal models, dental occlusion, cartilage, calcification, osteogenesis

[1]State Key Laboratory of Military Stomatology & National Clinical Research Center for Oral Diseases & Shaanxi International Joint Research Center for Oral Diseases, Department of Oral Anatomy and Physiology and TMD, School of Stomatology, the Fourth Military Medical University, Xi'an, China
[2]Key Laboratory of Shaanxi Province for Craniofacial Precision Medicine Research, Department of Implant Dentistry, College of Stomatology, Xi'an Jiaotong University, Xi'an, China
[3]Center for Advancing Materials Performance from the Nanoscale (CAMP-Nano) & Hysitron Applied Research Center in China (HARCC), State Key Laboratory for Mechanical Behavior of Materials, Xi'an Jiaotong University, Xi'an, China
[4]School of Biomedical Engineering, the Fourth Military Medical University, Xi'an, China
[5]Department of Mechanical Engineering, University of Delaware, Newark, DE, USA
[6]Department of Health Statistics, the Fourth Military Medical University, Xi'an, China
*Authors contributing equally to this work.

A supplemental appendix to this article is available online.

Corresponding Authors:
M. Wang, State Key Laboratory of Military Stomatology & National Clinical Research Center for Oral Diseases & Shaanxi International Joint Research Center for Oral Diseases, Department of Oral Anatomy and Physiology and TMD, School of Stomatology, Fourth Military Medical University, Changle West Road, Xi'an, 710032, China.
Email: mqwang@fmmu.edu.cn
Z. Shan, Center for Advancing Materials Performance from the Nanoscale (CAMP-Nano) & Hysitron Applied Research Center in China (HARCC), State Key Laboratory for Mechanical Behavior of Materials, Xi'an Jiaotong University, Xianning West Road, Xi'an, 710049, China.
Email: zwshan@mail.xjtu.edu.cn

Introduction

Osteoarthritis (OA) of diarthrodial joints, the most common form of arthritis, could be initiated by biomechanical causes such as the change of loading pattern (Moyer et al. 2014). The affected joint is often associated with the degeneration of the noncalcified articular cartilage, thickening of the calcified cartilage (Bobinac et al. 2003; Burr 2004; Aicher et al. 2014), and remodeling of the subchondral bone, which involves not only trabecular bone but also subchondral cortical bone (Bobinac et al. 2003; Burr et al. 2012; Goldring et al. 2016). The main histological change of subchondral trabecular bone is bone volume loss at an early stage but increases later (Burr et al. 2012; Zhen et al. 2013), while the change of subchondral cortical bone is consistent thickening, which is often mixed with the thickening of the calcified cartilage (Gordon et al. 1984; Burr 2004). In fact, the term *osteochondral interface*, in which the histological tidemark is located, is often used to represent the region that covers the calcified cartilage and subchondral cortical bone (Burr 2004; Yuan et al. 2014). Mineralization of the osteochondral interface often increases with age and altered loading conditions, and it likely plays a key role in the development of OA (Oegema et al. 1997; Burr et al. 2012). Most investigations of OA joints have focused on the articular cartilage or subchondral trabecular bone. Little is known about the remodeling of the osteochondral interface during OA progression, especially its role at the early stage of OA.

The temporomandibular joint (TMJ), a frequent OA involvement site, is biomechanically related to dental occlusion (Wang et al. 2009). This makes it easy to interrupt the TMJ biomechanical environment by altering dental occlusion via orthodontic and prosthodontic treatments without invasive operation in TMJs. Based on this, we recently developed a unilateral anterior crossbite (UAC) rodent model via installing a pair of metal tubes onto the animal's incisors. OA-like lesions such as cartilage decay (Zhang et al. 2013; Liu et al. 2014; Wang et al. 2014; Lu et al. 2015; Liu et al. 2016) and subchondral trabecular bone loss (Liu et al. 2014; Yang et al. 2014; Lu et al. 2015; Yang et al. 2015; Liu et al. 2016) were observed in the TMJs after UAC operation. Impressively, we disclosed contribution of the decay of deep-zone cartilage to the thickening of the calcified cartilage (Zhang et al. 2016). This implies an increased stiffness of the osteochondral interface that has yet to be verified. We recently reported that targeting subchondral bone by strontium, NF-kB essential modulator binding domain (NBD) peptide, norepinephrine, and so on is helpful to rescue the UAC-stimulated OA-like lesions, including those at the osteochondral interface (Jiao et al. 2016; Liu et al. 2016). It seems that there is an involvement of subchondral cortical bone formation in addition to the cartilage calcification at the osteochondral interface in the UAC TMJs, which has yet to be demonstrated. Furthermore, it is of clinical interest whether the changes at the osteochondral interface are radiologically detectable, which could serve as an imaging diagnostic target for OA.

In the present study, we performed a longitudinal biochemical and mechanical evaluation of the osteochondral interface in the TMJs of UAC rats. Morphology information was obtained using both in vivo and ex vivo assays. Dynamic mechanical analysis (DMA) at the nano level was performed to track the change in mechanical properties. We found that the osteochondral interface in the TMJ, including deep-zone cartilage and subchondral cortical bone, was sensitive to a joint mechanical environment, shown by the significant changes in thickness, density, and stiffness. Although the environment of the cartilage and subchondral bone could be changed due to the stiffness of the interface, whether or not the stiffened interface would accelerate OA progress remains to be confirmed. With that evidence, the osteochondral interface could be a new diagnostic and therapeutic target of mechanically initiated OA in the TMJ.

Materials and Methods

Animal Model

Ninety female and 36 male Sprague-Dawley rats at 6 wk old were obtained from the Animal Center of the Fourth Military Medical University. All procedures and administration for the animals were approved by the University Ethics Committee and performed according to the institutional guidelines. Animals were randomly assigned to control and experimental groups (Appendix Table 1). In UAC groups, the aberrant prosthesis was applied as described previously (Wang et al. 2014). For 3 female rats in each subgroup, calcein (5 mg/kg; Sigma) solution was injected intraperitoneally at 14 d before rats were killed. All rats received the same standardized diet throughout the procedure.

Animals were euthanized at 4, 12, or 20 wk after surgery. Our previous data indicated that no differences in degrading changes were found between the left- and right-side TMJs in the UAC rats (unpublished data, Appendix Fig. 3) and mice (Lu et al. 2015). For both the male and female rats, the left TMJ tissue blocks of 6 rats in each subgroup were used for histological analysis, including hematoxylin and eosin (H&E) or Safranin O staining ($n = 6$). The right TMJ condyles were immediately immersed into icy saline for visual inspection ($n = 6$). The bilateral condyles of 3 female rats with calcein injection were fixed in 2.5% glutaraldehyde for 48 h, dehydrated in ethanol, and embedded in a mixture of methyl methacrylate and dibutyl phthalate. Samples were sectioned into 100-μm slices using a hard tissue slicer (SP1600; Leica). Sections of the left condyle were stained by von Kossa reagents (GMS80045; Baoman Biotech) for osteochondral interface thickness measurement ($n = 3$, Appendix Methods), and those of the right condyle were inspected under a fluorescent microscope to analyze mineralization of the interface. For the other 6 female rats without calcein injection, the left condyles were fixed in 4% paraformaldehyde for micro–computed tomography (CT) scanning ($n = 6$, Appendix Methods), and the right condyles were prepared for the nano–dynamic mechanical analysis (DMA) test ($n = 6$, Appendix Methods).

Results

Condylar Deformation and Cartilage Degradation of the UAC Rats

In the control group, the TMJ condylar head was plump spindle shaped with a smooth articular surface. Four weeks after UAC operation, the condyle head still kept the shape of a spindle but became slim, indicating the width of the condyle head had decreased and looked like a gangly spindle (Fig. 1A). At 12 wk, the condyle of the UAC rat exhibited a slight deformation and further changed into a "gourd" shape at 20 wk (Fig. 1A). Three-way classification analysis indicated that the factors of treatment and time showed a significant effect on the value of the macroscopic score (both $P < 0.001$), while the factor of sex showed no effect ($P = 0.779$). The interaction of sex and group showed a nonsignificant effect ($P = 0.779$), while the interaction of sex and time, as well as group and time, showed a significant effect ($P < 0.001$). The macroscopic scores of the UAC group were higher than the age-matched controls at all 3 timepoints (all $P < 0.05$, Fig. 1B). The scores of female UAC rats at 20 wk were higher than those at 4 and 12 wk ($P < 0.001$), while the scores of male UAC rats at 12 and 20 wk were higher than those at 4 wk ($P = 0.001$). The scores of male UAC rats were much higher than those of the female UAC rats at 12 wk ($P = 0.004$) but were lower than the scores of female rats at 20 wk ($P = 0.017$).

Degeneration of condylar cartilage was obvious (Fig. 2A) in the UAC rats, similar to previous studies on mice (Liu et al. 2014; Lu et al. 2015; Liu et al. 2016). As we previously reported, few inflammatory cells were observed in the cartilage. Three-way classification analysis indicated that both treatment and time (both $P < 0.001$) showed significant effects on the value of modified Osteoarthritis Research Society International (OARSI) histomorphology score, while sex showed no effect ($P = 0.083$). The interaction of sex and group, sex and time, and group and time showed a nonsignificant effect (all $P > 0.05$). The modified OARSI histological score in the UAC group was higher than the age-matched control at all 3 timepoints (all $P < 0.05$, Fig. 2B). We then used females only for the following detections.

Osteochondral Interface Mineralization

The osteochondral interface shown by von Kossa staining, including the calcified cartilage and subchondral cortical bone, was thicker in 12- and 20-wk UAC rats than in the age-matched controls evaluated by the ratio of the osteochondral interface to the noncalcified cartilage (Fig. 3A, B). The subchondral bone displayed a strengthened neomineralization, as shown by the in vivo fluorescence assay (Fig. 3C). In the 4- and 12-wk control rats, neomineralization occurred far from the osteochondral interface (green, Fig. 3C). In the control rats at 20 wk, it appeared close to the osteochondral interface. In UAC rats, however, at 12 and 20 wk after UAC, there was much more significant mineralization than in the control group, shown as green stripes at the deep boundary of the osteochondral interface (arrowheads,
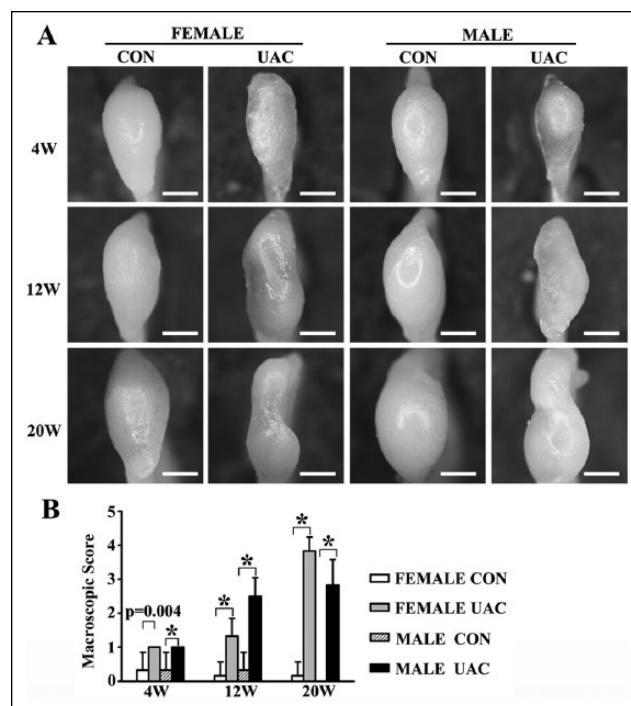

Figure 1. The gross appearance and morphological score of temporomandibular joint condyles. The condylar deformation appeared at 4 wk after UAC operation and deteriorated with time (**A**). The macroscopic scores of the UAC group were higher than the age-matched controls at all 3 timepoints (**B**). Bars = 1 mm. CON, control group; UAC, unilateral crossbite group; 4W, 4 wk; 12W, 12 wk; 20W, 20 wk. *$P < 0.001$. Note: The value of male CON groups at 20 wk equals 0.

Fig. 3C). This observation was confirmed by the gray-scale intensity measured by the Matlab processing program (Appendix Fig. 2). The fluorescent intensity of the 4-wk UAC group was low, similar to those in the 4- and 12-wk control groups.

According to the micro-CT images, the size of condyle head was reduced in the UAC rats. The length in the anterior-posterior direction was shorter at all 3 timepoints than the corresponding control group. Decreased width in the medial-lateral direction was found significant in UAC rats at 12 wk (all $P < 0.05$, Fig. 4B). The structure of the osteochondral interface altered gradually with age in the control group, was porous at 4 wk, but was "cortex-like" as a plate at 12 and 20 wk (Fig. 4A). In the UAC group, however, the cortex-like plate structure appeared at 4 wk, and the density increased over time (Fig. 4A). Bone mineral density (BMD) of the osteochondral interface in UAC rats was higher than the matched controls starting from 12 wk ($P < 0.05$, Fig. 4C). In contrast to the enhanced ossification at the osteochondral interface, UAC rats showed a significant loss of subchondral trabecular bone at 4 and 12 wk (Fig. 4D), as characterized by the decreased bone volume fraction (BV/TV) and increased trabecular separation (Tb.Sp) (all $P < 0.05$, Fig. 4D). In comparison to the control group, the trabecular number (Tb.N) and trabecular thickness (Tb.Th) in UAC rats were lower at 4 and 12 wk, respectively (both $P < 0.001$, Fig. 4D). This subchondral trabecular bone loss ceased
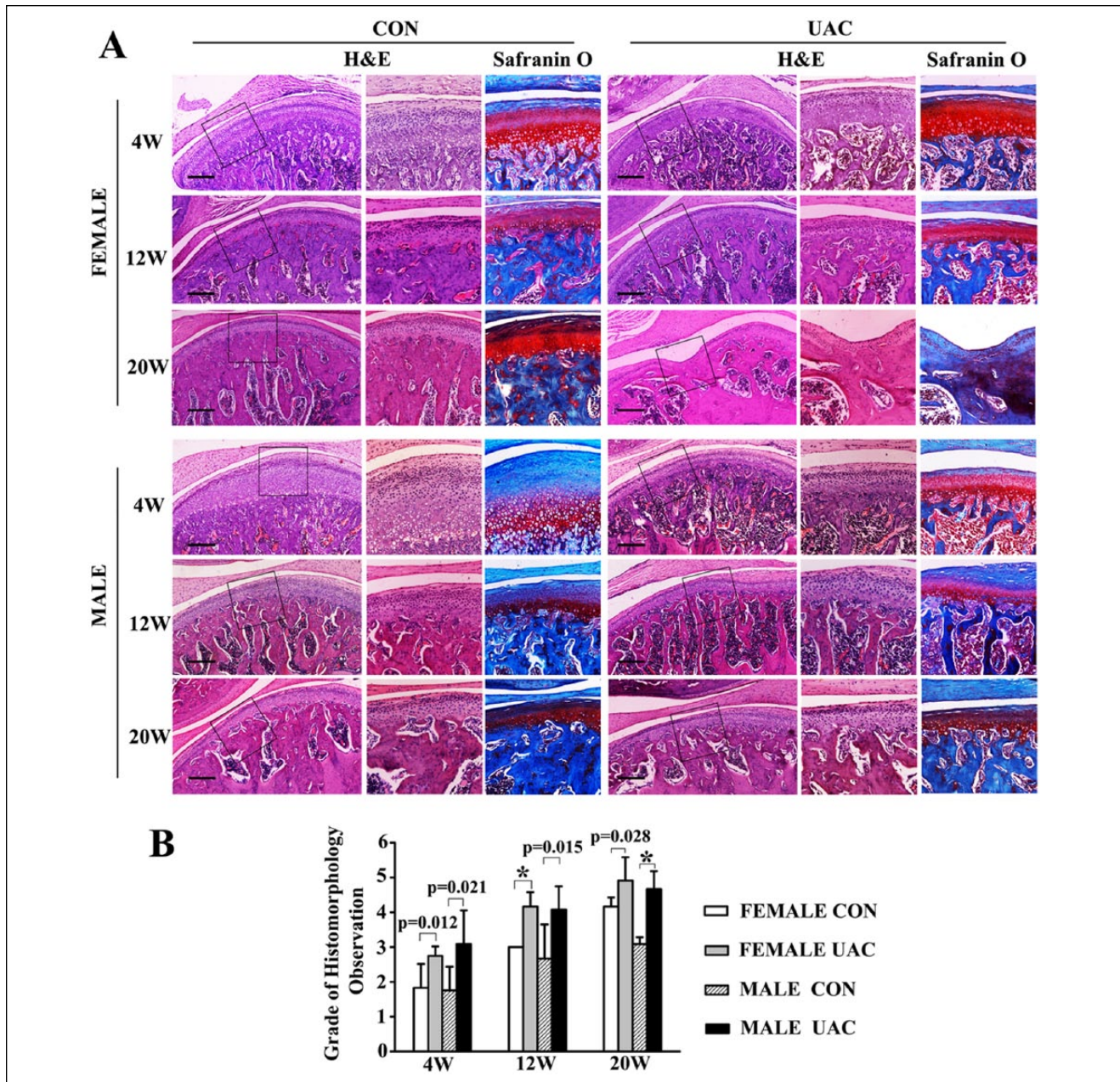
Figure 2. Hematoxylin and eosin (H&E) and Safranin O staining and modified Osteoarthritis Research Society International (OARSI) score of temporomandibular joint condyles. Degeneration of condylar cartilage was obvious in the UAC rats (**A**). The modified OARSI histological score in the UAC group was higher than the age-matched control at all 3 timepoints (**B**). Bars = 300 μm. CON, control group; UAC, unilateral crossbite group; 4W, 4 wk; 12W, 12 wk; 20W, 20 wk. *$P < 0.001$.

with time. At 20 wk, the UAC and control rats had no detectable difference in all the trabecular bone parameters (all $P > 0.05$, Fig. 4D).

Stiffness of the Osteochondral Interface

Nano-DMA was performed to measure the mechanical properties of the osteochondral interface region. The complex modulus and tan delta were calculated based on the storage and the loss modulus. Results showed that the complex modulus, representing the resistance capability to compressive loading, increased in 12- and 20-wk UAC groups in comparison to the controls (all $P < 0.05$, Fig. 5A). Tan delta, which describes the energy transmission efficiency, was identical between the UAC and control groups at all timepoints (all $P > 0.05$, Fig. 5A). Besides the osteochondral interface region, the subchondral trabecular bone was also tested with nano-DMA. As expected, there was no change in mechanical properties of
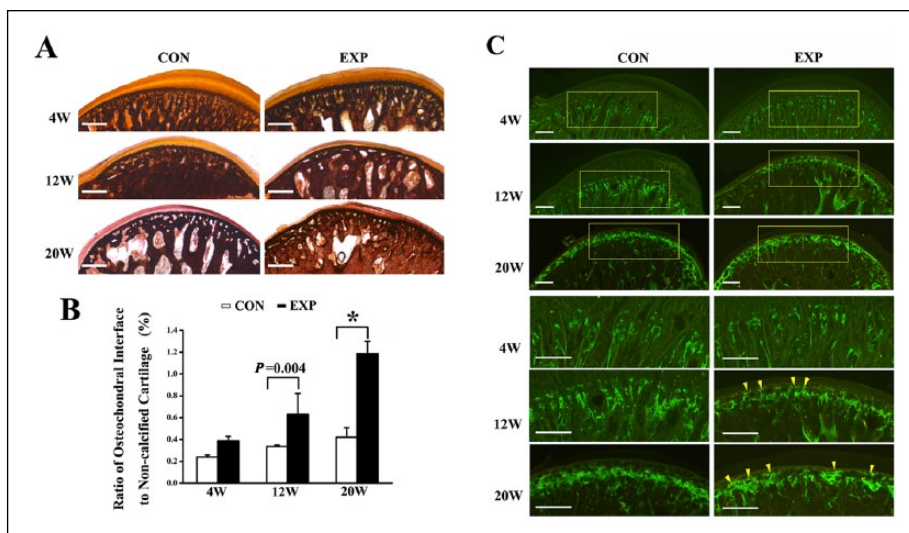
Figure 3. The von Kossa staining and the in vivo fluorescence assay of the osteochondral interface. The osteochondral interface shown by von Kossa staining included the calcified cartilage and subchondral cortical bone (**A**). The thickness ratio of the osteochondral interface to the noncalcified cartilage in the UAC condyle was higher than the control group at 12 and 20 wk (**B**). The neomineralization of subchondral bone, shown by in vivo calcein labeling (**C**). In UAC rats, at 12 and 20 wk after UAC, there was much more significant mineralization than in the control group, shown as green stripes at the deep boundary of the osteochondral interface (arrowheads, C). Bars = 300 μm. CON, control group; UAC, unilateral crossbite group; 4W, 4 wk; 12W, 12 wk; 20W, 20 wk. *$P < 0.001$.

bone tissue in the UAC groups at all timepoints (all $P > 0.05$, Fig. 5B).

As the rat masticatory frequency is 4 to 5 Hz (Liu et al. 1998), we specifically analyzed the mechanical properties at 4.53 Hz. The complex modulus of the osteochondral interface increased at 12 and 20 wk in the UAC group (both $P < 0.05$, Fig. 5A), while trabecular bone did not show any significant difference at the 3 timepoints (all $P > 0.05$, Fig. 5B). The Pearson correlation test showed a tendency ($r = 0.857$; $P < 0.05$) for the value of the complex modulus to increase in the osteochondral interface region as the value of BMD increased.

Discussion

In this study, we focused on the early stage detectability and progression of dental-originated TMJ OA-like lesions at the osteochondral interface using our developed UAC rat model. Presently, we found the ossification of osteochondral interface was due to the progressive deep-zone cartilage calcification (Zhang et al. 2016) and subchondral bone mineralization, which were characterized by the BMD enhancement observed on micro-CT images and the thickness increasing via von Kossa staining analysis. These loading-induced remodeling responses were stabilized by wk 20. We identified for the first time that the density and mechanical stiffness of the thickened osteochondral interface increased over time at the early stage of UAC stimulation.

The factor of sex showed a general similar trend on the TMJ OA lesions, but based on the present score values, the histological deformation of male UAC rats' condyles progressed more

rapidly (4 to 12 wk) than that of the female rats and entered the stable period earlier (12 to 20 wk), while that of the female UAC rats drastically deteriorated from 12 wk and became much heavier than that of the male rats at 20 wk. Regarding the OA scoring system, in knee OA, there is symptomatic OA and radiographic OA (Bedson et al. 2008). The present UAC-induced rat TMJ lesions are at most radiologic OA. Several score systems have been introduced in the literature and are almost exclusively dedicated to the evaluation of knee joint OA (Mankin et al. 1971; Ostergaard et al. 1997; Pritzker et al. 2006). However, a direct application of the scoring systems of the knee joint to the TMJ is inappropriate. Different from the hyaline cartilage in the knee joint, the TMJ condyle is covered by fibrous cartilage, which is critical for the tissue to support the gliding load during chewing (Ruggiero et al. 2015). The histological difference of the articular surface may contribute to the different surface changes between knee joint OA and TMJ OA. Knee joint OA in animal models usually involves an ulcerous surface (Custers et al. 2007). In contrast, the articular surface of the TMJ condyle with UAC-induced OA-like lesions has remained intact without obvious ulcer, abrasion, vertical fissures, or denudation (Wang et al. 2014). Therefore, it is necessary to modify the OARSI scoring system for the evaluation of TMJ OA (Appendix Table 3), in which the weight of ulcer surface is reduced.

Although the articular surface of the UAC rat TMJ condyle remained intact, the twisted spindle condyle in the 20-wk female UAC group was characteristic. This could be correlated with the alteration of deep-zone cartilage. Our histological morphology analysis indicated that the local shrinking region had no hypertrophic or prehypertrophic chondrocytes (Fig. 2A). Locally, the compact bone substituted the cancellous bone and was in direct contact with the fibrous superficial zone cartilage. The black belt showed by the histological slices with von Kossa staining (Fig. 3A) included the calcified cartilage as we previously reported (Zhang et al. 2016) and the freshly formed subchondral cortical bone disclosed by the in vivo calcein labeling. Although double labeling will provide more information on the amount of dynamic bone formation by measuring the distance between the 2 labels on, for example, the bone trabecula, the present aim of calcein labeling was to observe the distribution of neomineralization in the condylar subchondral interface region where the bone branched greatly. We indeed found that in UAC rats, the neomineralization was
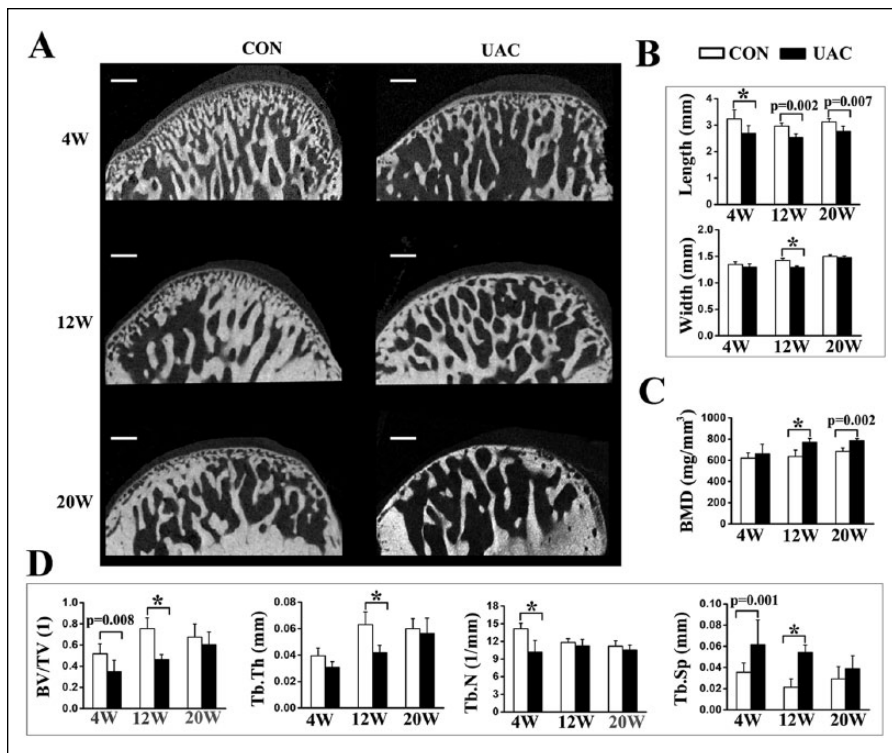
Figure 4. The micro–computed tomography images and bone histomorphology parameters of temporomandibular joint condyles. The structure of the osteochondral interface altered gradually with age in the control group, was porous at 4 wk, but was "cortex-like" as a plate at 12 and 20 wk. In the UAC group, the cortex-like plate structure appeared at 4 wk, and the density increased over time (**A**). The length in the anterior-posterior direction and width in the medial-lateral direction of the condylar head (**B**). Bone mineral density (BMD) of the osteochondral interface in UAC rats was higher than the matched controls starting from 12 wk (**C**). UAC rats showed significant loss of subchondral trabecular bone at 4 and 12 wk (**D**). Bars = 300 μm. BV/TV, bone volume fraction; CON, control group; Tb.N, trabecular number; Tb.Sp, trabecular separation; Tb.Th, trabecular thickness; UAC, unilateral crossbite group; 4W, 4 wk; 12W, 12 wk; 20W, 20 wk. *$P < 0.001$.

located much closer to the boundary of the osteochondral interface and was more significant in UAC rats than in the controls. In a previous study, we noticed upregulated bone formation capability in UAC rats (Yang et al. 2015). The region displayed subchondral trabecular bone loss, which was mediated by osteoclasts, as we disclosed previously (Yang et al. 2015), and was located away from the interface. This means that in this rat UAC model, the site where the osteoblasts mediated subchondral cortical bone formation was not coupled with the site where the osteoclasts mediated bone resorption, while they were coupled in daily bone remodeling activities (Maeda et al. 2012). The uncoupling of them could cause cartilage degeneration as indicated in mice with Camurati-Engelmann disease (CED) (Tang et al. 2009; Jiao et al. 2014). It is then rational to use drug targeting on subchondral bone remodeling as a way to rescue the OA-like lesions in UAC rats as reported previously (Jiao et al. 2016; Liu et al. 2016).

The DMA technique has been used to study the mechanical properties of biological tissue such as articular cartilage and bone (Tanaka et al. 2006; Fulcher et al. 2009; Mardas et al. 2012; Espino et al. 2014; Mardas et al. 2015). The TMJ is under dynamic loading during chewing (Palla et al. 2003), and the frequency of rat chewing is 4 to 5 Hz (Liu et al. 1998). As a result, we used 3.10 to 9.65 Hz to mimic the chewing frequency of rats, which was similar to other studies examining the mechanical properties of porcine TMJ cartilage and disk (Tanaka et al. 2003, 2006). DMA at nanoscale was adopted in the current study because of the small size of rats' TMJ condyle, especially the osteochondral interface. The theoretical model and the data-processing methods of nano-DMA are similar to DMA, as previously reported (Tanaka et al. 2006; Mardas et al. 2012; Espino et al. 2014; Mardas et al. 2015). To diminish the influence of the fixation treatment on the mechanical property, we air-dried the samples, which was similar to other studies that explored the mechanical properties of bovine bones using the DMA technique (Mardas et al. 2012, 2015). This made the locations of the detection sites observable. Both the articular cartilage and bone tissue contain collagens and proteoglycans, the intermolecular friction of which contributes to viscoelastic behavior without the fluid phase through a flow-independent mechanism (Stolz et al. 2004; Lu et al. 2009). However, the air-drying of the samples made the present in vitro data further incomparable with the in vivo conditions. We used the age-matched controls with the same sampling and detection methods. The complex modulus of the osteochondral interface in UAC condyles was significantly increased from 12 wk compared with the age-matched controls, which was consistent with the increased BMD. In contrast, the complex modulus of trabecular bone in UAC condyles had no significant difference with the controls indicated that the architecture of subchondral trabecular bone changed rather than the mechanical properties.

The increased densification of the subchondral plate in a sheep tibia increases stress in the deeper cartilage (Burr 2004). Also, the thickened subchondral cortical bone contributes to the decreased underlying cancellous bone mass and cartilage thinning (Ko et al. 2013). Similarly, in this study, UAC rats showed degradation of cartilage and loss of subchondral trabecular bone, accompanied by increased density, thickness, and stiffness of the osteochondral interface in the TMJ. It is suggested that the increased stiffness of osteochondral interface changes contributed to bone remodeling and cartilage degeneration. The new balance seemed reestablished in the
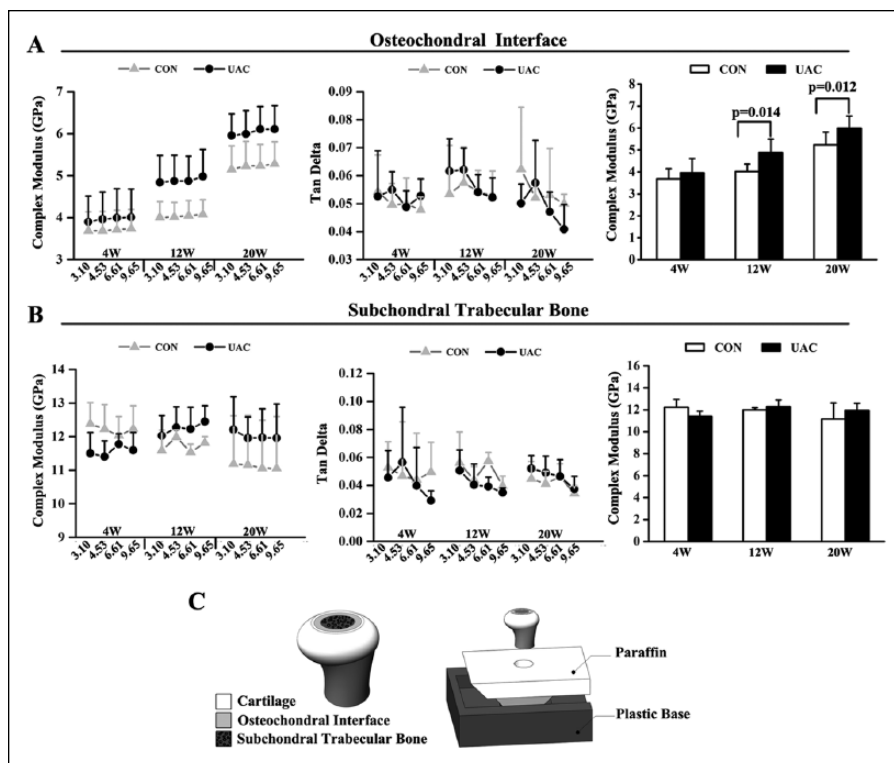
Figure 5. The mechanical property of osteochondral interface and subchondral trabecular bone using nano–dynamic mechanical analysis (DMA). The complex modulus increased in 12- and 20-wk UAC groups in comparison to the controls. Tan delta was identical between the UAC and control groups at all 3 timepoints (**A**). No change in mechanical properties existed in the bone tissue in the UAC groups at 3 timepoints (**B**). The complex modulus of the osteochondral interface at 4.53 Hz increased at 12 and 20 wk in the UAC group (A), while trabecular bone did not show any significant difference at 3 timepoints (B). CON, control group; UAC, unilateral crossbite group; 4W, 4 wk; 12W, 12 wk; 20W, 20 wk.

current UAC rats when cartilage calcification and subchondral bone loss ceased at 20 wk.

The present study proved that aberrant biomechanical stimulation could lead to thickening of the osteochondral interface via enhanced cartilage calcification at the superior region and unregulated bone formation at the inferior region of the osteochondral interface. Although the environment of the cartilage and subchondral bone could be changed due to the stiffness of the interface, whether or not the stiffened interface would accelerate OA progress remains to be confirmed. With that evidence, the osteochondral interface could be a new diagnostic and therapeutic target of the mechanically initiated OA in the TMJ.

Author Contributions

J. Zhang, contributed to conception, design, and data interpretation, drafted and critically revised the manuscript; L. Liao, J. Zhu, M. Xie, contributed to data acquisition, analysis, and interpretation, drafted the manuscript; X. Wan, contributed to data acquisition and analysis, drafted the manuscript; H. Zhang, contributed to data acquisition and analysis, critically revised the manuscript; M. Zhang, S. Yu, X.L. Lu, C. Chen, contributed to data analysis and interpretation, critically revised the manuscript; L. Lu, contributed to data acquisition and interpretation, critically revised the manuscript;

H. Yang, Z. Shan, contributed to data acquisition, analysis, and interpretation, critically revised the manuscript; D. Jing, X. Liu, contributed to conception, critically revised the manuscript; M. Wang, contributed to conception and design, critically revised the manuscript. All authors gave final approval and agree to be accountable for all aspects of the work.

ORCID iD

M. Wang [ID] http://orcid.org/0000 -0002-7373-385X

References

Aicher WK, Rolauffs B. 2014. The spatial organisation of joint surface chondrocytes: review of its potential roles in tissue functioning, disease and early, preclinical diagnosis of osteoarthritis. Ann Rheum Dis. 73(4):645–653.

Bedson J, Croft PR. 2008. The discordance between clinical and radiographic knee osteoarthritis: a systematic search and summary of the literature. BMC Musculoskelet Disord. 9:116.

Bobinac D, Spanjol J, Zoricic S, Maric I. 2003. Changes in articular cartilage and subchondral bone histomorphometry in osteoarthritic knee joints in humans. Bone. 32(3):284–290.

Burr DB. 2004. Anatomy and physiology of the mineralized tissues: role in the pathogenesis of osteoarthrosis. Osteoarthritis Cartilage. 12 Suppl A:20S–30S.

Burr DB, Gallant MA. 2012. Bone remodelling in osteoarthritis. Nat Rev Rheumatol. 8(11):665–773.

Custers RJ, Creemers LB, Verbout AJ, van Rijen MH, Dhert WJ, Saris DB. 2007. Reliability, reproducibility and variability of the traditional Histologic/Histochemical Grading System vs the new OARSI Osteoarthritis Cartilage Histopathology Assessment System. Osteoarthritis Cartilage. 15(11):1241–1248.

Espino DM, Shepherd DE, Hukins DW. 2014. Viscoelastic properties of bovine knee joint articular cartilage: dependency on thickness and loading frequency. BMC Musculoskelet Disord. 15:205.

Fulcher GR, Hukins DW, Shepherd DE. 2009. Viscoelastic properties of bovine articular cartilage attached to subchondral bone at high frequencies. BMC Musculoskelet Disord. 10:61.

Goldring SR, Goldring MB. 2016. Changes in the osteochondral unit during osteoarthritis: structure, function and cartilage-bone crosstalk. Nat Rev Rheumatol. 12(11):632–644.

Gordon GV, Villanueva T, Schumacher HR, Gohel V. 1984. Autopsy study correlating degree of osteoarthritis, synovitis and evidence of articular calcification. J Rheumatol. 11(5):681–686.

Jiao K, Zeng G, Niu LN, Yang HX, Ren GT, Xu XY, Li FF, Tay FR, Wang MQ. 2016. Activation of α2A-adrenergic signal transduction in chondrocytes promotes degenerative remodelling of temporomandibular joint. Sci Rep. 6:30085.

Jiao K, Zhang M, Niu L, Yu S, Zhen G, Xian L, Yu B, Yang K, Liu P, Cao X, et al. 2014. Overexpressed TGF-β in subchondral bone leads to mandibular condyle degradation. J Dent Res. 93(2):140–147.

Ko FC, Dragomir C, Plumb DA, Goldring SR, Wright TM, Goldring MB, van der Meulen MC. 2013. In vivo cyclic compression causes cartilage degeneration and subchondral bone changes in mouse tibiae. Arthritis Rheum. 65(6):1569–1578.

Liu YD, Liao LF, Zhang HY, Lu L, Jiao K, Zhang M, Zhang J, He JJ, Wu YP, Chen D, et al. 2014. Reducing dietary loading decreases mouse temporomandibular joint degradation induced by anterior crossbite prosthesis. Osteoarthritis Cartilage. 22(2):302–312.

Liu YD, Yang HX, Liao LF, Jiao K, Zhang HY, Lu L, Zhang M, Zhang J, He JJ, Wu YP, et al. 2016. Systemic administration of strontium or NBD peptide ameliorates early stage cartilage degradation of mouse mandibular condyles. Osteoarthritis Cartilage. 24(1):178–187.

Liu ZJ, Ikeda K, Harada S, Kasahara Y, Ito G. 1998. Functional properties of jaw and tongue muscles in rats fed a liquid diet after being weaned. J Dent Res. 77(2):366–376.

Lu L, Zhang X, Zhang M, Zhang H, Liao L, Yang T, Zhang J, Xian L, Chen D, Wang M. 2015. RANTES and SDF-1 are keys in cell-based therapy of TMJ osteoarthritis. J Dent Res. 94(11):1601–1609.

Lu XL, Mow VC, Guo XE. 2009. Proteoglycans and mechanical behavior of condylar cartilage. J Dent Res. 88(3):244–248.

Maeda K, Kobayashi Y, Udagawa N, Uehara S, Ishihara A, Mizoguchi T, Kikuchi Y, Takada I, Kato S, Kani S, et al. 2012. Wnt5a-Ror2 signaling between osteoblast-lineage cells and osteoclast precursors enhances osteoclastogenesis. Nat Med. 18(3):405–412.

Mankin HJ, Dorfman H, Lippiello L, Zarins A. 1971. Biochemical and metabolic abnormalities in articular cartilage from osteo-arthritic human hips. II. Correlation of morphology with biochemical and metabolic data. J Bone Joint Surg Am. 53(3):523–537.

Mardas M, Kubisz L, Biskupski P, Mielcarek S. 2015. Time-dependent changes in dynamic mechanical properties of irradiated bone. Biomed Mater Eng. 25(4):397–403.

Mardas M, Kubisz L, Biskupski P, Mielcarek S, Stelmach-Mardas M, Kaluska I. 2012. Radiation sterilized bone response to dynamic loading. Mater Sci Eng C Mater Biol Appl. 32(6):1548–1553.

Moyer RF, Ratneswaran A, Beier F, Birmingham TB. 2014. Osteoarthritis year in review 2014: mechanics—basic and clinical studies in osteoarthritis. Osteoarthritis Cartilage. 22(12):1989–2002.

Oegema TJ Jr, Carpenter RJ, Hofmeister F, Thompson RJ Jr. 1997. The interaction of the zone of calcified cartilage and subchondral bone in osteoarthritis. Microsc Res Tech. 37(4):324–332.

Ostergaard K, Petersen J, Andersen CB, Bendtzen K, Salter DM. 1997. Histologic/histochemical grading system for osteoarthritic articular cartilage: reproducibility and validity. Arthritis Rheum. 40(10):1766–1771.

Palla S, Gallo LM, Gossi D. 2003. Dynamic stereometry of the temporomandibular joint. Orthod Craniofac Res. 6(Suppl 1):37–47.

Pritzker KP, Gay S, Jimenez SA, Ostergaard K, Pelletier JP, Revell PA, Salter D, van den Berg WB. 2006. Osteoarthritis cartilage histopathology: grading and staging. Osteoarthritis Cartilage. 14(1):13–29.

Ruggiero L, Zimmerman BK, Park M, Han L, Wang L, Burris DL, Lu XL. 2015. Roles of the fibrous superficial zone in the mechanical behavior of TMJ Condylar Cartilage. Ann Biomed Eng. 43(11):2652–2662.

Stolz M, Raiteri R, Daniels AU, VanLandingham MR, Baschong W, Aebi U. 2004. Dynamic elastic modulus of porcine articular cartilage determined at two different levels of tissue organization by indentation-type atomic force microscopy. Biophys J. 86(5):3269–3283.

Tanaka E, Kikuzaki M, Hanaoka K, Tanaka M, Sasaki A, Kawai N, Ishino Y, Takeuchi M, Tanne K. 2003. Dynamic compressive properties of porcine temporomandibular joint disc. Eur J Oral Sci. 111(5):434–439.

Tanaka E, Yamano E, Dalla-Bona DA, Watanabe M, Inubushi T, Shirakura M, Sano R, Takahashi K, van Eijden T, Tanne K. 2006. Dynamic compressive properties of the mandibular condylar cartilage. J Dent Res. 85(6):571–575.

Tang Y, Wu X, Lei W, Pang L, Wan C, Shi Z, Zhao L, Nagy TR, Peng X, Hu J, et al. 2009. TGF-beta1-induced migration of bone mesenchymal stem cells couples bone resorption with formation. Nat Med. 15(7):757–765.

Wang MQ, Xue F, He JJ, Chen JH, Chen CS, Raustia A. 2009. Missing posterior teeth and risk of temporomandibular disorders. J Dent Res. 88(10):942–945.

Wang YL, Zhang J, Zhang M, Lu L, Wang X, Guo M, Zhang X, Wang MQ. 2014. Cartilage degradation in temporomandibular joint induced by unilateral anterior crossbite prosthesis. Oral Dis. 20(3):301–306.

Yang T, Zhang J, Cao Y, Zhang M, Jing L, Jiao K, Yu S, Chang W, Chen D, Wang M. 2015. Wnt5a/Ror2 mediates temporomandibular joint subchondral bone remodeling. J Dent Res. 94(6):803–812.

Yang T, Zhang J, Cao Y, Zhang M, Jing L, Jiao K, Yu S, Wang M. 2014. Decreased bone marrow stromal cells activity involves in unilateral anterior crossbite-induced early subchondral bone loss of temporomandibular joints. Arch Oral Biol. 59(9):962–969.

Yuan XL, Meng HY, Wang YC, Peng J, Guo QY, Wang AY, Lu SB. 2014. Bone-cartilage interface crosstalk in osteoarthritis: potential pathways and future therapeutic strategies. Osteoarthritis Cartilage. 22(8):1077–1089.

Zhang M, Wang H, Zhang J, Zhang H, Yang H, Wan X, Jing L, Lu L, Liu X, Yu S, et al. 2016. Unilateral anterior crossbite induces aberrant mineral deposition in degenerative temporomandibular cartilage in rats. Osteoarthritis Cartilage. 24(5):921–931.

Zhang X, Dai J, Lu L, Zhang J, Zhang M, Wang Y, Guo M, Wang X, Wang M. 2013. Experimentally created unilateral anterior crossbite induces a degenerative ossification phenotype in mandibular condyle of growing Sprague-Dawley rats. J Oral Rehabil. 40(7):500–508.

Zhen G, Wen C, Jia X, Li Y, Crane JL, Mears SC, Askin FB, Frassica FJ, Chang W, Yao J, et al. 2013. Inhibition of TGF-β signaling in mesenchymal stem cells of subchondral bone attenuates osteoarthritis. Nat Med. 19(6):704–712.